Abstract

We use the principle of adiabatic invariance of the action to find semiclassically the rotational fine structure of asymmetric top molecules. We show that by adiabatically switching the moments of inertia of a prolate or oblate symmetric top molecule, we may determine the asymmetric top energy levels even when crossing a separatrix boundary.

Rotational adiabatic switching of asymmetric top molecules

Chris W. Patterson
Theoretical Division, Los Alamos National Laboratory, Los Alamos, New Mexico 87545

R. Scott Smith and Randall B. Shirts
Department of Chemistry, University of Utah, Salt Lake City, Utah 84112

(Received 29 August 1986; accepted 9 September 1986)

We use the principle of adiabatic invariance of the action to find semiclassically the rotational fine structure of asymmetric top molecules. We show that by adiabatically switching the moments of inertia of a prolate or oblate symmetric top molecule, we may determine the asymmetric top energy levels even when crossing a separatrix boundary.

INTRODUCTION

In this paper we determine the rotational fine structure of a model asymmetric top molecule by adiabatically switching[1-5] the moments of inertia of a prolate or oblate symmetric top molecule. Physically, such an adiabatic switching could correspond to a very floppy molecule with slow "vibrational" motion or to reactive scattering with slowly changing coordinates at a barrier. In this paper, however, we emphasize the adiabatic switching as a useful technique in itself to determine the energy levels of an asymmetric top molecule without the need to diagonalize the rotational Hamiltonian. This technique can be extended to the case of rotational–vibrational coupling where such diagonalizations become computationally intractable.

The Hamiltonian of an asymmetric top molecule is given simply in terms of the body fixed components of the angular momentum

$$H = CJ_x^2 + BJ_y^2 + AJ_z^2 , \tag{1}$$

where we let $\hbar = 1$ and the rotational constants are given in terms of the principal moments of inertia by

$$A = (1/2I_{xx}) , \quad B = (1/2I_{yy}) , \quad \text{and} \quad C = (1/2I_{zz}) . \tag{2}$$

It is standard convention to define the principal axes of a molecule such that $A \geqslant B \geqslant C$. A molecule is a prolate symmetric top when $B = C$ and is an oblate symmetric top when $B = A$.

It is convenient to parametrize the angular momentum in the body-fixed frame in terms of Euler angles with respect to the laboratory frame with **J** along the lab z axis such that[6]

$$J_x = -J \sin\beta \cos\gamma , \tag{3a}$$

$$J_y = J \sin\beta \sin\gamma , \tag{3b}$$

$$J_z = J \cos\beta \equiv J_\gamma , \tag{3c}$$

where the Euler angles of the body coordinates with respect to the lab are $(-\gamma, -\beta)$. With this parametrization, the Hamiltonian becomes

$$H(J_\gamma,\gamma) = C(J^2 - J_\gamma^2)\cos^2\gamma + B(J^2 - J_\gamma^2)\sin^2\gamma + AJ_\gamma^2 , \tag{4}$$

where J^2 is a constant of the motion. Thus our Hamiltonian has only one dimension with two degrees of freedom. This is because our original Hamiltonian in three dimensions had two constants of the motion: the total angular momentum J and its projection on the lab axis $J_z \equiv M$. The simple form of Eq. (4) results from the implicit condition $J = M$.

In Fig. 1 we plot the rotational energy (RE) surface for a most symmetric top where $B = (A + C)/2$ with J fixed at $J = 10$. We use spherical coordinates with the energy plotted radially as a function of angles (β,γ). The contours of constant energy which define this surface correspond to the classical trajectories of the Hamiltonian.

For the above Hamiltonian, the equations of motion are

$$\dot{\gamma} = \frac{\partial H}{\partial J_\gamma} , \tag{5a}$$

$$\dot{J}_\gamma = -\frac{\partial H}{\partial \gamma} . \tag{5b}$$

From these equations, we may find the fixed points of the RE surface in Fig. 1 where $\dot{\gamma} = 0$ and $\dot{J}_\gamma = 0$. We find stable fixed points for $\beta = 0, \pi$ corresponding to the $\pm J_z$ axes and for $\gamma = 0, \pi$ and $\beta = \pi/2$ corresponding to the $\pm J_x$ axes. We find saddle points or unstable fixed points for $\gamma = \pm \pi/2$ and $\beta = \pi/2$ corresponding to the $\pm J_y$ axes. The J_y axis is unstable because, by definition, it is the axis with the intermediate moment of inertia I_{yy}.

The trajectory which goes through the J_y axis is called the separatrix and corresponds to energy $E = BJ^2$. The se-

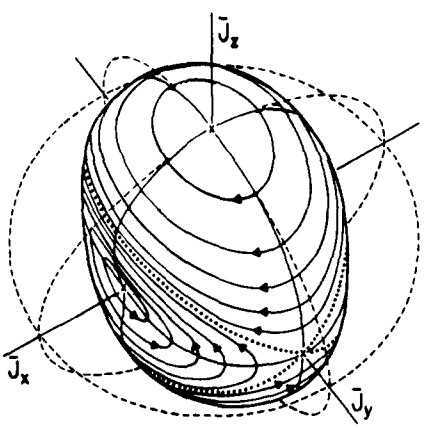

FIG. 1. Rotational energy surface. The energy contours for this most asymmetric top with $B = (A + C)/2$ correspond to the semiclassical trajectories for $J = 10$. The separatrix is shown with a dotted line and the fixed points are denoted with an $\times$.

 0021-9606/86/247241-04$02.10

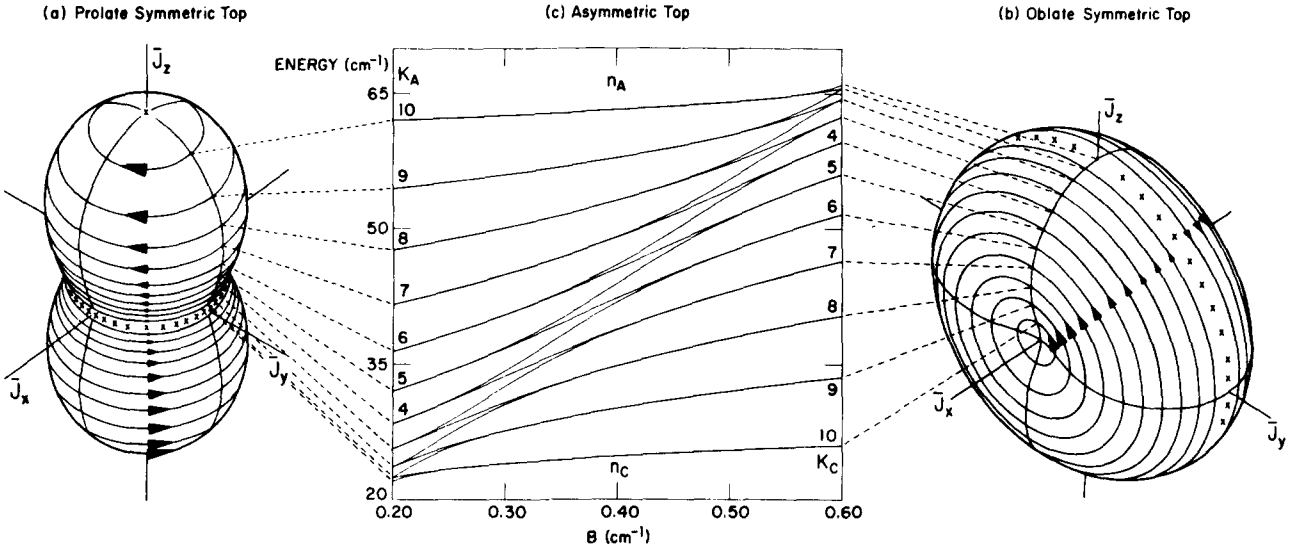

FIG. 2. Energy correlation diagram for an asymmetric top. (a) RE surface for a prolate symmetric top with $B = C = 0.2\ \mathrm{cm}^{-1}$ and (b) RE surface for a oblate symmetric top with $B = A = 0.6\ \mathrm{cm}^{-1}$. The $J = 10$ asymmetric top quantum energy levels are shown in (b) as a function of the rotational constant B. The corresponding semiclassical trajectories in the prolate and oblate limit where K_A and K_C are good quantum numbers are shown in (a) and (b). For arbitrary B the quantum levels are labeled with n_A and n_C. When $B = 0.4\ \mathrm{cm}^{-1}$ the RE surface is shown in Fig. 1.

paratrix separates motion around the J_z and J_x stable fixed points as shown in Fig. 1. By substituting the energy BJ^2 for H in Eq. (4), one finds that the separatrix is two circles on the RE surface intersecting at the $\pm J_y$ axis and going through the $J_x - J_z$ plane ($\gamma = 0$) at angles β_s and $\pi - \beta_s$ where

$$\beta_s = \cos^{-1}\sqrt{\frac{B-C}{A-C}}. \tag{6}$$

In the prolate top limit where $B = C$, the separatrix merges with the $J_z = 0$ plane forming a locus of stable fixed points. In the oblate top limit where $B = A$ the separatrix merges with the $J_x = 0$ plane again forming a locus of stable fixed points. Such stable fixed points for the prolate and oblate RE surfaces are denoted with a $\times$ in Figs. 2(a) and 2(b), respectively.

In the prolate and oblate limit, semiclassical quantization is straightforward. Substituting $B = C$ in Eq. (4), we find the Hamiltonian for the prolate symmetric top,

$$H(J_\gamma) = CJ^2 + (A - C)J_\gamma^2, \tag{7}$$

is independent of γ so that $J_\gamma = J_z \equiv K_A$ is a constant of the motion.

The semiclassical quantization condition for the action,

$$S_z = \int_0^{2\pi} J_\gamma(z\ \text{axis})d\gamma = 2\pi n_A, \tag{8}$$

for precessional orbits about J_z result in the quantization

$$|K_A| = n_A \quad \text{for } n_A = J, J-1, \ldots, 0 \tag{9}$$

for prolate symmetric tops. The energies levels are doubly degenerate corresponding to trajectories with K_A quantized about the $\pm J_z$ axis as shown in Fig. 2(a). Note that we may reverse the roles of the J_z and J_x axis in the Hamiltonian in Eq. (4) by exchanging A and C. The Hamiltonian for an oblate symmetric top then becomes

$$H(J_\gamma) = AJ^2 - (A - C)J_\gamma^2 \tag{10}$$

so that $J_\gamma = J_x \equiv K_C$ is now a constant of the motion. The semiclassical quantization for the action now becomes

$$S_x = \int_0^{2\pi} J_\gamma(x\ \text{axis})d\gamma = 2\pi n_C \tag{11}$$

for precessional orbits about J_x result in the quantization

$$|K_C| = n_C \quad \text{for } n_C = J, J-1, \ldots, 0 \tag{12}$$

for oblate symmetric tops. Again, the energies levels are doubly degenerate corresponding to trajectories with K_c quantized about the $\pm J_x$ axis as shown in Fig. 2(b). Equations (8) and (11) are the correct semiclassical quantizations for precessional trajectories of the asymmetric top even when J_z and J_x are not conserved. However, rather than use these equations to find the semiclassical energies for the general asymmetric top,[6,7] we shall use the principle of adiabatic invariance of the action.

First, in Fig. 2(c), we show the quantum energies for $J = 10$ by diagonalizing H in Eq. (4) as a function of the rotational constant B. This diagonalization is readily accomplished in the $2J + 1$ basis set (J,K_C) or (J,K_A). We use rotational constants of a model "heavy" molecular top with $C = 0.2\ \mathrm{cm}^{-1}$ and $A = 0.6\ \mathrm{cm}^{-1}$. The trajectories on the RE surfaces for the prolate and oblate symmetric tops in Figs. 2(a) and 2(b) are correlated with the quantum energies on the extreme left and right of the energy diagram in Fig. 2 where $B = C$ and $B = A$, respectively. Note that each degenerate pair of n_A energy levels in the prolate limit in Fig. 2(c) is correlated with a nondegenerate pair $n_C = (J - n_A, J - n_A - 1)$ in the oblate limit and visa versa. Thus the action quantum numbers (n_A,n_C) in Eqs. (8) and (11) uniquely label an asymmetric top quantum state even when K_A and K_C are not good quantum numbers and J_z and J_x are not conserved.

ADIABATIC SWITCHING

We now try to duplicate the quantum energies of the asymmetric top in Fig. 2(c) by adiabatic switching the rotational constant B starting with the prolate or oblate symmetric top limit where the quantized trajectories are known. If the rotational constant B is changed slowly for such an initial prolate or oblate top trajectory, the action must be conserved in this one-dimensional system. Thus if one starts a trajectory with the properly quantized action, the action will remain quantized, and the resultant trajectory will necessarily remain the semiclassically correct one until the separatrix is crossed.[2] We solve Hamilton's equations in Eq. (5) with the prolate symmetric top initial conditions $K_A = J, J-1, \ldots, 0$ with $B = C$ and follow the resulting adiabatic energies given by Eq. (4) as B is gradually increased. In Fig. 3(a) the semiclassical energies with dashed lines are compared with the quantum energies with solid lines. Similarly for the oblate symmetric top, we use the initial conditions $K_C = J, J-1, \ldots, 0$ with $B = A$ and follow the resulting adiabatic energies in Fig. 3(b) as B is gradually decreased. The switching times over the full range of B is the same for all $J+1 = 11$ trajectories and corresponds to ~ 30 periods of the longest period $K_C = 1$ or $K_A = 1$ trajectories. The lower K_C or K_A trajectories will be the first to violate the adiabatic conditions with faster switching times since they have the longest period trajectories.

It is clear that before the trajectories cross the separatrix, the semiclassical energies shown in Fig. 3 are quite accurate. We use the semiclassical correspondence $J^2 \rightarrow (J+1/2)^2$ in Eq. (4) rather than the more accurate $J^2 \rightarrow J(J+1)$ for the reasons discussed below. It is evident in Fig. 3 that the energy of the separatrix BJ^2 is a linear function of B. It is readily seen in Fig. 3 that the exact energies are symmetric about the separatrix with respect to exchange of K_A and K_C. The action at the separatrix determines the number of allowed semiclassical precessional trajectories about the J_z and J_x axes. The action of the separatrix about the J_z axis is

$$S_z = \int_0^{2\pi} J_\gamma(z \text{ axis}) d\gamma \geqslant 2\pi n_A , \tag{13}$$

where we solve for J_γ in Eq. (4) with $H = BJ^2$. We find that

$$n_A \leqslant 2J\beta_s/\pi \tag{14}$$

so that the number of semiclassical trajectories around the J_z axis depends linearly on the separatrix angle β_s given in Eq. (6). Similarly, the number of semiclassical trajectories around the J_x axis is

$$n_C \leqslant 2J(\pi/2 - \beta_s)/\pi = J - 2J\beta_s/\pi . \tag{15}$$

The separatrix itself corresponds to a semiclassical trajectory where $\beta_s = n\pi/2J$ and n is an integer. Note that when $B = (A+C)/2$ for the "most" asymmetric top, we have $\beta_s = \pi/4$ and $n_C, n_A \leqslant J/2$. That is, half of the semiclassical trajectories are oblate and half are prolate as shown in Fig. 1. When J is an even integer, the separatrix itself is a semiclassical trajectory. In Fig. 1 we show the $2J+1 = 21$ semiclassical trajectories on the RE surface for a most asymmetric top. Note in Fig. 1 that the precessional trajectories about the J_x axis appear as librational trajectories when viewed about the J_z axes and visa versa.

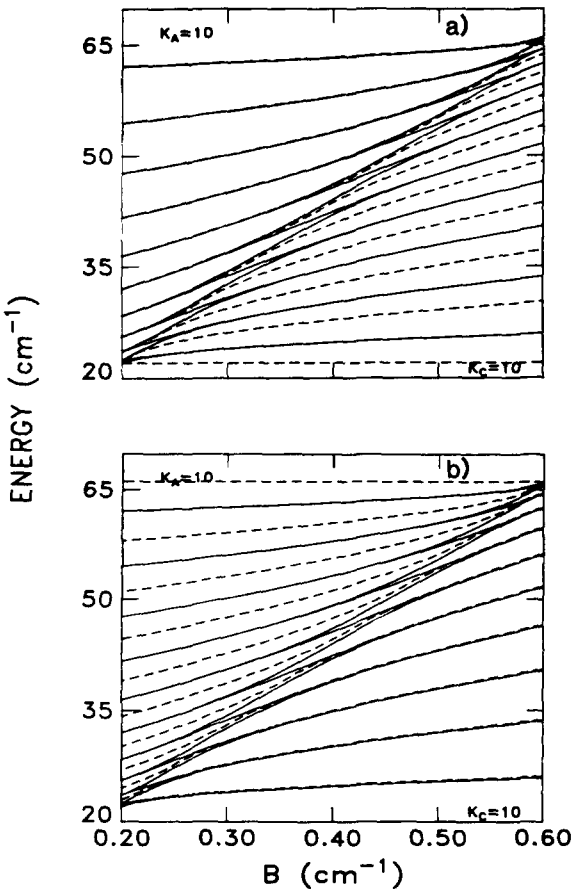

FIG. 3. Comparison of semiclassical and quantum energy levels for an asymmetric top with $J = 10$. The semiclassical energy levels are found by adiabatically switching (a) using initial prolate symmetric top trajectories with $B = 0.2\,\text{cm}^{-1}$ and K_A = integer and (b) using initial oblate symmetric top trajectories with $B = 0.6\,\text{cm}^{-1}$ and K_C = integer. After the separatrix crossing at energy BJ^2 the semiclassical energies are no longer accurate. For the librational trajectories after the separatrix crossing, half-integer quantum numbers can be used to obtain accurate semiclassical energies.

In Fig. 4 we follow the classical trajectory of the $K_A = 5$ level in Fig. 3(a) for various values of B. The action for these trajectories is simply the area under the curves. It is found that this action is always 10π to any desired degree of accuracy by slowing the switching time. As expected, the action is conserved even when crossing the separatrix boundary. Note that after crossing the separatrix the precessional trajectories appear librational about the $J_\gamma = J_z$ axis. The trajectory in Fig. 4(c) corresponds to $B \cong (A+C)/2$ and is very near the separatrix. Thus it is almost touching the unstable fixed points at $\pm J_y$ where $\gamma = \pi/2$ or $3\pi/2$ and $J_\gamma = 0$. When the separatrix is crossed, half of the classical trajectories will cross near the $+J_y$ hyperbolic fixed point and end up in precessional trajectories about the $+J_x$ axis, while the other half of the trajectories will cross near the $-J_y$ axis and end up in precessional trajectories about the $-J_x$ axis, depending on the phase of initial trajectory. For the particular trajectory shown in Fig. 4, the separatrix was crossed near $-J_y$ at $\gamma = 3\pi/2$ resulting in a precessional trajectory about the $-J_x$ axis where $\gamma = \pi$. Note that these

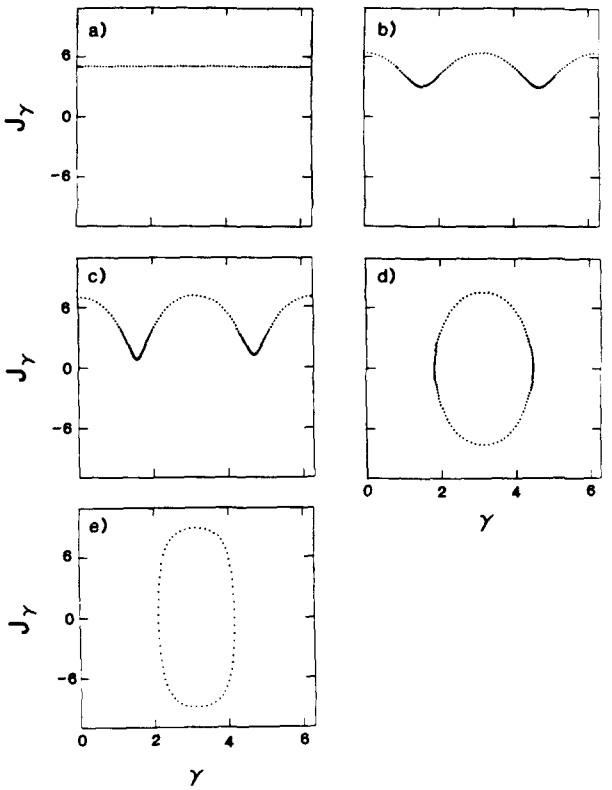

FIG. 4. Phase space plots of a $J = 10$ classical trajectory of an asymmetric top resulting from adiabatically switching the rotational constant B (in cm^{-1}) where (a) $B \cong C = 0.2$, (b) $B \cong 0.3$, (c) $B \cong 0.4$, (d) $B \cong 0.5$, and (e) $B \cong A = 0.6$. Since $J_Y \equiv J_z$, the trajectories in (a), (b), and (c) precess about the J_z axis and the trajectories in (d) and (e) precess about the $-J_x$ axis. The trajectory starts in (a) with $K_A = 5$ and finishes in (e) with $K_C = 5.5$. In (c) the trajectory is near the separatrix of Fig. 1 and spends most of the time near the $\pm J_y$ unstable fixed points.

trajectories about $-J_x$ in Figs. 4(d) and 4(e) appear librational since $J_Y = J_z$.

At the separatrix the quantum splitting of the K_A and K_C levels becomes large due to tunneling across the separatrix as described in Ref. 6. After the separatrix crossing, the classical energies no longer follow their quantum counterparts in Fig. 3. This is because the semiclassical conditions for the action in Eqs. (8) and (11) assume that the trajectories are precessional rather than librational. However, when the separatrix is crossed, we must change our quantization conditions to account for the librational trajectories. As shown by Colwell *et al.*[7] this can be accomplished by letting $n_A \rightarrow n_A + 1/2$ in Eq. (8) when crossing the separatrix in Fig. 3(a), and $n_C \rightarrow n_C + 1/2$ in Eq. (11) when crossing the separatrix in Fig. 3(b). That is, for librational trajectories there are two turning points and half-integers must be used for the semiclassical quantization. This is only valid if we use the semiclassical condition $J \rightarrow J + 1/2$. We then have the correlations

$$(n_A + 1/2) \rightarrow (J + 1/2) - n_C \quad (n_A, n_C = \text{integer}), \tag{16a}$$

$$(n_C + 1/2) \rightarrow (J + 1/2) - n_A \quad (n_A, n_C = \text{integer}) \tag{16b}$$

between half-integer and integer quantum numbers when crossing the separatrix.

CONCLUSIONS

From the above considerations, we see that Fig. 3(a) is equivalent to adiabatically switching from the oblate symmetric top limit starting with half-integer quantization. With this prescription, we arrive at the correct prolate energies after the separatrix has been crossed. Similarly, Fig. 3(b) is equivalent to adiabatically switching from the prolate symmetric top limit starting with half-integer quantization to obtain the correct oblate energies after the separatrix has been crossed. In both cases the action is conserved, but we have now started with an action appropriate for the librational trajectories which occur after the separatrix has been crossed.

It is appropriate to discuss how these results may be applied to practical problems. It is always possible to diagonalize the $2J + 1$ dimensional Hamiltonian matrix to obtain rotational energies, but in cases where J is very large, or where full diagonalization is not desirable, one may obtain energy levels for the asymmetric top using the above method of adiabatic switching. For a given final value of B, one may either switch from the oblate or prolate limits. For those values of K_A and K_C for which the final energy is less than BJ^2, half-integer quantization should be used in switching from the prolate limit or integer quantization should be used in swtiching from the oblate limit. For those values of K_A and K_C for which the final energy is greater than BJ^2, integer quantization should be used when switching from the prolate limit or half-integer quantization should be used in switching from the oblate limit. This will assure accurate quantum eigenvalues for all values of K_A and K_C except possibly those very close to the separatrix. Tunneling corrections[6] could be included for these states if more accurate values were desired.

ACKNOWLEDGMENTS

The contribution by CWP was supported by the U.S. Department of Energy and the contributions by RSS and RBS was supported by the Associated Western Universities (an agency of DOE) and by NSF Grant No. CHE 85-11164.

[1] E. A. Solov'ev, Sov. Phys. JETP **48**, 635 (1978).
[2] R. T. Skodje, F. Borondo, and W. P. Reinhardt, J. Chem. Phys. **82**, 4611 (1985).
[3] R. T. Skodje and F. Borondo, Chem. Phys. Lett. **118**, 409 (1985).
[4] B. R. Johnson, J. Chem. Phys. **83**, 1204 (1985).
[5] C. W. Patterson, J. Chem. Phys. **83**, 4618 (1985).
[6] W. G. Harter and C. W. Patterson, J. Chem. Phys. **80**, 4241 (1980).
[7] S. M. Colwell, N. C. Handy, and W. H. Miller, J. Chem. Phys. **68**, 745 (1978).